Renewable and Sustainable Energy Reviews 16 (2012) 5747–5759

Contents lists available at SciVerse ScienceDirect

Renewable and Sustainable Energy Reviews

journal homepage: www.elsevier.com/locate/rser

Dynamic output-feedback wide area damping control of HVDC transmission considering signal time-varying delay for stability enhancement of interconnected power systems

Yong Li [a,b], Fang Liu [c,d,*], Christian Rehtanz [b], Longfu Luo [a], Yijia Cao [a]

[a] College of Electrical and Information Engineering, Hunan University, Changsha, China
[b] Institute of Energy Systems, Energy Efficiency and Energy Economics, TU Dortmund University, Dortmund, Germany
[c] School of Information Science and Engineering, Central South University, Changsha, China
[d] Graduate School of Environment and Energy Engineering, Waseda University, Tokyo, Japan

A R T I C L E I N F O

Article history:
Received 24 May 2011
Received in revised form
6 May 2012
Accepted 8 May 2012
Available online 4 August 2012

Keywords:
Dynamic output-feedback (DOF) controller
High-voltage direct current (HVDC) transmission
Lyapunov function
Varying-delay
Wide area damping control (WADC)

A B S T R A C T

In this paper, an output-feedback-type wide area damping control (WADC) strategy is presented as a supplementary control of high-voltage direct current (HVDC) transmission to enhance thestability of large-scale interconnected power systems. This strategy can effectively suppress the varying-delay effects of wide area signal on the damping performance. A discrete-time system model that considers the varying-delay feature of wide area signal is established, then a dynamic output-feedback (DOF) type WADC is formulated by employing a new stabilization analysis method based on Lyapunov function. All the solutions of controller design problems are converted into the framework of linear matrix inequalities (LMIs). Compared to the conventional design method, the varying-delay of wide area signal is involved during each step of controller design, which is advantage to eliminate the effects of signal varying-delay on damping performance. Both the four-machine two-area test system and the sixteen-machine five-area interconnected system are used to validate the control concept and the designed controller.

© 2012 Elsevier Ltd. All rights reserved.

1. Introduction

Nowadays more and more high-voltage direct current (HVDC) transmissions are being applied in power systems for long-distance power transmission and interconnection of electric networks. As a backbone interconnected line, HVDC transmission plays an effective role on system operating performance. It can

* Corresponding author.
E-mail address: csuleon@gmail.com (F. Liu).

1364-0321/$ - see front matter © 2012 Elsevier Ltd. All rights reserved.
http://dx.doi.org/10.1016/j.rser.2012.05.015

Nomenclature

CCL	cone complementary linearization
DOF	dynamic output-feedback
FACTS	flexible AC transmission system
HLF	high-pass filter
HVDC	high-voltage direct current
LFO	low-frequency oscillations
LMIs	linear matrix inequalities
NETS	New England Test System
NYPS	New York Power System
WAC	wide area control
WADC	wide area damping control
WAMS	wide area measurement system
PSS	power system stabilizer
SS	state-space
SOF	static output-feedback
TF	transfer-function
$x(k)$	state vector
$u(k)$	control-input
$y(k)$	control-output
A	system matrix
B	input matrix
C_d	output matrix with delay effect
$d(k)$	time-varying delay
A_c,B_c,C_c,D_c	state-space matrices of DOF controller
$\tilde{K}_{SOF}$	control gain of SOF controller
P,L	real matrix
Q_i $(i=1,2,3)$	real matrix
Z_j,R_j $(j=1,2)$	real matrix
X,Y,N,S,M	real matrix

contribute transmission capacity increase, power flow regulation, and stability enhancement for interconnected power system [1–3]. Meanwhile, with the technical development of synchronized phasor measurement, wide area measurement system (WAMS) gets more and more application in large-scale power system [4,5]. WAMS can not only realize global state estimation for power system, but also be construct wide area control (WAC) strategy by introducing wide area signals [6].

In large-scale interconnected systems, such as the European interconnected networks [7], America interconnected systems [4], and power grids of China [8], inter-area oscillations among different areas are easily excited by disturbances, faults or changes of system operating condition. This kind of low-frequency oscillations (LFO) generally represent the interaction among various generators located in different areas, and further represent the power oscillations on backbone interconnected lines, thus inevitably endanger the stability and security of system.

In recent years, several control methods were proposed to prevent LFO, such as the wide area power system stabilizer (PSS) [9] located at the generation side, and the flexible AC transmission system (FACTS) devices [10,11] placed at the transmission or the distribution sides. In practice, HVDC transmission is generally used as a backbone line in large-scale interconnected systems. It is able to naturally enhance system stability. Further, if the supplementary control function of HVDC transmission is developed to construct oscillation damping strategy where the control-input is provided by WAMS, then the so-called HVDC wide area damping control (WADC) strategy could contribute to the effective LFO damping effectively and thus improve the overall stability of interconnected system.

However, the delay effect of wide area signals should be considered carefully for the WAC strategy. During the period of signal transmission and processing, it inevitably leads to a certain delay for wide area signals. Due to the technical development of WAMS, the time delay can be controlled in a relatively small value such as 300 ms, but it still affects even destroys the control performance [9,12], especially on the practical situation the delay is not constant but time-varying. To overcome this problem, some control methods that consider the delay effect were proposed [9,13]. In fact, power system with the application of WAMS can be looked as a delay-dependent system defined in the field of control theory [14,15]. It is feasible to employ advanced control theories or methods to solve the delay effects of wide area signals, and design an advanced controller to fundamentally suppress delay effects.

In this paper, a dynamic output-feedback (DOF) WADC for HVDC transmission will be proposed. The hybrid HVDC/AC interconnected system will be linearized as a discrete-time model with the varying-delay feature of wide area signal. Further the control problem will be formulated as a solution of linear matrix inequalities (LMIs). Both the four-machine two-area test system and the sixteen-machine five-area interconnected system will be used to validate this control design method.

2. Description of HVDC wide area damping control

Fig. 1 shows the basic structure of HVDC WADC strategy. The rectifier side has a local pole controller and a wide area controller which are used to implement the constant DC current control and the oscillation damping control, respectively. The WADC is in fact a supplementary control of HVDC local pole control, which has some features as follows:

- To get a good damping performance, the WADC chooses remote variable (e.g., current or power flow on the tie-line) as the control-input signal. The signal choice satisfies the observability/controllability index based on modal analysis (e.g., residues analysis method [16]).
- The important part of WADC is the dynamic output-feedback control matrix K_{DOF}. Unlike the traditional control gain of output-feedback control, the K_{DOF} is not a constant value but has a state-space (SS) or a transfer-function (TF) representation. It can provide phase compensation for the concerned LFO mode as well as delay compensation for the wide area signal.
- The high-pass filter (HPF) is used to preprocess the control signal and retain the concerned LFO mode that should be damped. The time-constant T_{wh} selects 10 s according to the experience [17].

In general, the objective of HVDC DOF-WADC is to damp LFO especially the inter-area oscillations in power systems and at the same time ensure the required control performance of the HVDC local pole controller.

3. Controller design considering time-varying delay of wide area signal

3.1. Linearized discrete-time model with time-varying delay

The linearized discrete-time model, which takes the time-varying delay of wide area signal into consideration, can be

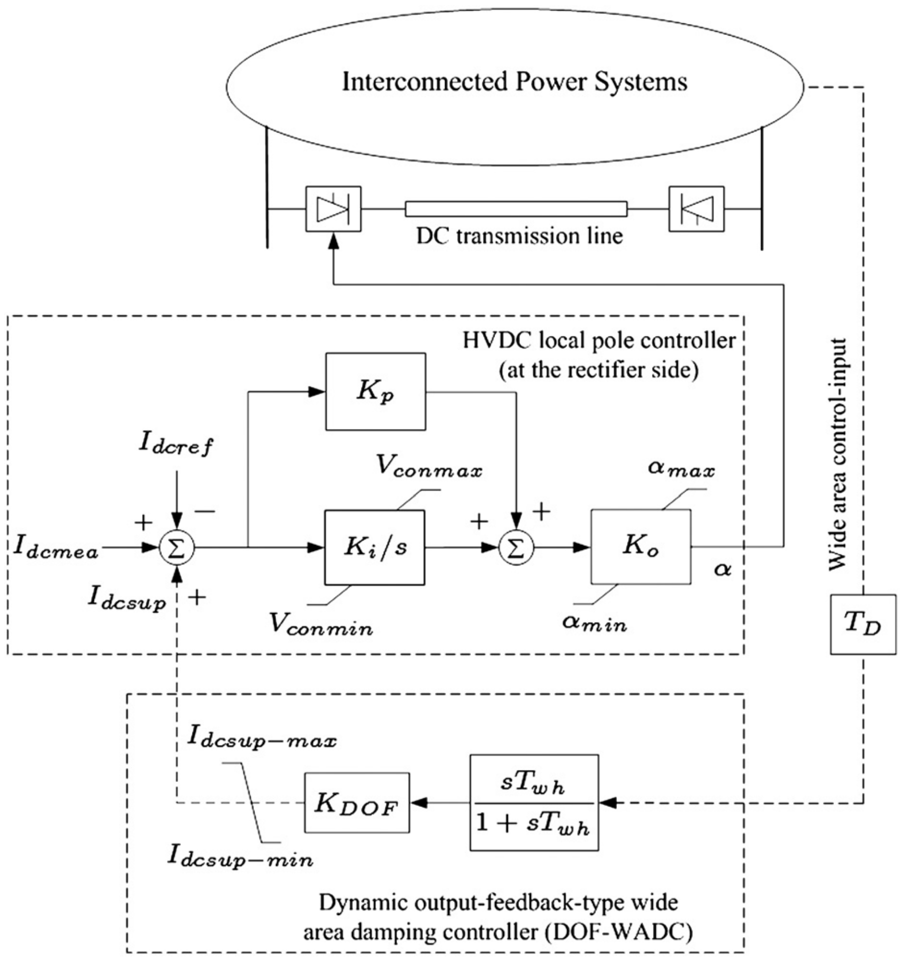


Fig. 1. Basic structure of HVDC wide area damping control.

represented as

$$\begin{cases} x(k+1)=Ax(k)+Bu(k), \\ y(k)=C_d x(k-d(k)), \\ x(k)=\varphi(k), \quad -d_2 \le k \le 0, \end{cases} \tag{1}$$

where $x(k)$ is the state vector; $u(k)$ and $y(k)$ are the wide area control-output and -input, respectively; A, B, and C_d are the system, the input and the output matrices, respectively; $d(k)$ is the time-varying delay that satisfies

$$d_1 \le d_k \le d_2. \tag{2}$$

The DOF controller can be represented as follows:

$$\begin{bmatrix} x_c(k+1) \\ u(k) \end{bmatrix} = \begin{bmatrix} A_c & B_c \\ C_c & D_c \end{bmatrix} \begin{bmatrix} x_c(k-d(k)) \\ y(k) \end{bmatrix}, \tag{3}$$

where $x_c(k)$ is the state vector of DOF controller; A_c, B_c, C_c, and D_c are the real matrices.

Under the action of (3), the open-loop system (1) yields a closed-loop system as follows:

$$\xi(k+1)=\tilde{A}\xi(k)+\tilde{B}_d\xi(k-d(k)), \tag{4}$$

where

$$\xi(k)=\begin{bmatrix} x^T(k) \\ x_c^T(k) \end{bmatrix}, \quad \tilde{A}=\begin{bmatrix} A & 0 \\ 0 & 0 \end{bmatrix}, \quad \tilde{B}_d=\begin{bmatrix} BD_cC_d & BC_c \\ B_cC_d & A_c \end{bmatrix}.$$

The $\tilde{B}_d$ in (4) can be further described as

$$\tilde{B}_d=\begin{bmatrix} B & 0 \\ 0 & I \end{bmatrix}\begin{bmatrix} D_c & C_c \\ B_c & A_c \end{bmatrix}\begin{bmatrix} C_d & 0 \\ 0 & I \end{bmatrix}=\begin{bmatrix} B & 0 \\ 0 & I \end{bmatrix}\tilde{K}_{SOF}\begin{bmatrix} C_d & 0 \\ 0 & I \end{bmatrix}.$$

The optimization of DOF controller in (3) is transformed into that of static output-feedback (SOF) controller $\tilde{K}_{SOF}$, that is

$$u(k)=\tilde{K}_{SOF}y(k)=\begin{bmatrix} D_c & C_c \\ B_c & A_c \end{bmatrix} y(k). \tag{5}$$

The aim of controller design is to find a suitable $\tilde{K}_{SOF}$ to ensure the closed-loop system (4) can be asymptotically stable even when the control signal has a certain time-varying delay.

3.2. Stabilization conditions

Currently, there are several stabilization analysis methods generalized in LMI framework [18]. However, these methods cannot solve the effects of time-varying delay on stabilization performance effectively. In this paper, based on free-weighting matrix method [15] developed recently for time delay system, a theorem will be derived to analyze the stability of the system (1) with time-varying delay of wide area signal.

Theorem. *For given scalars d_1 and d_2 with $d_2 > d_1 > 0$, system* (1) *with d_k satisfying* (2) *can be stabilized by* (3) *if there exist* $P=P^T>0$, $L=L^T>0$, $Q_i=Q_i^T>0$ $(i=1,\ 2,\ 3)$, $Z_j=Z_j^T>0$, $R_j=R_j^T>0$ $(j=1,\ 2)$, $X=\begin{bmatrix} X_{11} & X_{12} \\ X_{12}^T & X_{22} \end{bmatrix}\ge 0$, $Y=\begin{bmatrix} Y_{11} & Y_{12} \\ Y_{12}^T & Y_{22} \end{bmatrix}\ge 0$, $N=[N_1^T\ N_2^T]^T$, $S=[S_1^T\ S_2^T]^T$,

$M=[M_1^T\ M_2^T]^T$, and $\tilde{K}_{SOF}$ satisfies that

$$\psi(1)=\begin{bmatrix} X & N \\ N^T & Z_1 \end{bmatrix}\geq 0, \tag{6}$$

$$\psi(2)=\begin{bmatrix} Y & S \\ S^T & Z_2 \end{bmatrix}\geq 0, \tag{7}$$

$$\psi(3)=\begin{bmatrix} X+Y & M \\ M^T & Z_1+Z_2 \end{bmatrix}\geq 0, \tag{8}$$

$$PL=I,\quad Z_jR_j=I(j=1,2), \tag{9}$$

$$\begin{bmatrix} \phi & \Xi_1^T & d_2\Xi_2^T & d_{12}\Xi_2^T \\ \Xi_1 & -L & 0 & 0 \\ d_2\Xi_2 & 0 & -d_2R_1 & 0 \\ d_{12}\Xi_2 & 0 & 0 & -d_{12}R_2 \end{bmatrix}<0, \tag{10}$$

where

$$\phi=\begin{bmatrix} \phi_{11} & \phi_{12} & S_1 & -M_1 \\ \phi_{12}^T & \phi_{22} & S_2 & -M_2 \\ S_1^T & S_2^T & -Q_1 & 0 \\ -M_1^T & -M_2^T & 0 & -Q_2 \end{bmatrix},$$

$$\phi_{11}=Q_1+Q_2+(d_{12}+1)Q_3-P+N_1+N_1^T+d_2X_{11}+d_{12}Y_{11},$$

$$\phi_{12}=N_2^T-N_1+M_1-S_1+d_2X_{12}+d_{12}Y_{12},$$

$$\phi_{22}=-Q_3-N_2-N_2^T+M_2+M_2^T-S_2-S_2^T+d_2X_{22}+d_{12}Y_{22},$$

$$\Xi_1=[\tilde{A}\ \tilde{B}\tilde{K}_{SOF}\tilde{C}_d\ 0\ 0],$$

$$\Xi_2=[\tilde{A}-I\ \tilde{B}\tilde{K}_{SOF}\tilde{C}_d\ 0\ 0],$$

$$d_{12}=d_2-d_1.$$

Proof. Define

$$\eta(l)=\xi(l+1)-\xi(l). \tag{11}$$

It is clear from (11) that $\xi(k+1)=\xi(k)+\eta(k)$ and $\eta(k)=\xi(k+1)-\xi(k)$. Then, choose a Lyapunov functional candidate to be

$$\begin{cases} V(k)=V_1(k)+V_2(k)+V_3(k)+V_4(k), \\ V_1(k)=\xi^kP\xi(k), \\ V_2(k)=\sum_{i=k-d_1}^{k-1}\xi^T(i)Q_1\xi(i)+\sum_{i=k-d_2}^{k-1}\xi^T(i)Q_2\xi(i), \\ V_3(k)=\sum_{l=k-d_2}^{k-d_1}\sum_{i=l}^{k-1}\xi^T(i)Q_3\xi(i), \\ V_4(k)=\sum_{i=-d_2}^{-1}\sum_{l=k+i}^{k-1}\eta^T(i)Z_1\eta(i)+\sum_{i=-d_2}^{-d_1-1}\sum_{l=k+i}^{k-1}\eta^T(i)Z_2\eta(i), \end{cases} \tag{12}$$

where $P=P^T>0,Q_i=Q_i^T>0\ (i=1,2,3),Z_i=Z_i^T>0\ (i=1,2)$.

Defining $\Delta V(k)=V(k+1)-V(k)$, calculating the $\Delta V(k)$ along the system (1) and based on the free-weighting matrix method, following the similar analysis process in [15], it yields:

$$\Delta V(k)\leq\begin{pmatrix} \zeta^T(k)\{\phi+\Xi_1^TP\Xi_1+\Xi_2^T[d_2Z_1+d_{12}Z_2]\Xi_2\}\zeta(k) \\ -\sum_{l=k-d(k)}^{k-1}\zeta_2^T(k,l)\Psi_1\zeta_2(k,l)-\sum_{l=k-d_2}^{k-d(k)-1}\zeta_2^T(k,l)\Psi_2\zeta_2(k,l) \\ -\sum_{l=k-d(k)}^{k-d_1-1}\zeta_2^T(k,l)\Psi_3\zeta_2(k,l) \end{pmatrix},$$

where $\zeta(t)=[\xi^T(k)\xi^T(t-d(k))\xi^T(t-d_1)\xi^T(t-d_2)]^T$, $\zeta_1(k)=[\xi^T(k)\xi^T(t-\tau(k))]^T$, $\zeta_2(k)=[\zeta_1^T(k)\eta^T(l)]^T$.

Therefore, if $\Psi_i\geq 0(i=1,2,3)$ and $\phi+\Xi_1^TP\Xi_1+\Xi_2^T(d_2Z_1+d_{12}Z_2)\Xi_2>0$, then $\Delta V(k)<0$. By using Schur complements, it is found that $\phi+\Xi_1^TP\Xi_1+\Xi_2^T(d_2Z_1+d_{12}Z_2)\Xi_2>0$ is equal to

$$\begin{bmatrix} \phi & \Xi_1^TP & d_2\Xi_2^TZ_1 & d_{12}\Xi_2^TZ_2 \\ P^T\Xi_1 & -P & 0 & 0 \\ d_2Z_1^T\Xi_2 & 0 & -d_2Z_1 & 0 \\ d_{12}Z_2^T\Xi_2 & 0 & 0 & d_{12}Z_2 \end{bmatrix}<0. \tag{13}$$

For the inequality (13), pre- and post-multiplying its left and right sides by $diag\left\{I,P^{-1},Z_1^{-1},Z_2^{-1}\right\}$ yields

$$\begin{bmatrix} \phi & \Xi_1^T & d_2\Xi_2^T & d_{12}\Xi_2^T \\ \Xi_1 & -P^{-1} & 0 & 0 \\ d_2\Xi_2 & 0 & -d_2Z_1^{-1} & 0 \\ d_{12}\Xi_2 & 0 & 0 & d_{12}Z_2^{-1} \end{bmatrix}<0. \tag{14}$$

Defining $L=P^{-1}$, $R_i=Z_i^{-1}(i=1,2)$ in (14), it can be seen that (9) and (10) hold. Therefore, based on the above analysis, it can be concluded that if conditions (6)–(10) are satisfied, system (1) can be stabilized by the controller (3).

3.3. Optimization objective and iterative algorithm

Since there are some equality terms like (9) in the theorem, it is impossible to optimize the controller (5). To overcome this problem, the cone complementary linearization (CCL) algorithm [19] is used to transform the controller design into a nonlinear optimization problem as follows:

$$\text{Min. } Tr\left(PR+\sum_{j=1}^{2}Z_jR_j\right)$$

$$\text{s.t.}\begin{cases} (6)-(8),(10),\text{and} \\ \begin{bmatrix} P & I \\ I & P \end{bmatrix}\geq 0,\quad \begin{bmatrix} Z_j & I \\ I & R_j \end{bmatrix}\geq 0,\ j=1,2, \\ P>0,\quad L>0,\quad Q_i>0,\ i=1,2,3, \\ Z_j>0,\quad R_j>0,\ j=1,2. \end{cases} \tag{15}$$

The following iterative algorithm is planned to solve the above nonlinear optimization problem.

Algorithm.

- *Step*-1: Set the initial value $d_2>d_1$, the iteration step Δd and the iteration number N;
- *Step*-2: Find a set of initial values (P_0, L_0, Q_{i0}, Z_{j0}, R_{j0}, M_0, N_0, S_0, X_0, Y_0, $\tilde{K}_{SOF0}$) so that (15) can be held;
  Set $k=0$;
- *Step*-3: Solve the following optimization problem:

  $$\text{Min.}Tr\left(P_kL+PL_k+\sum_{j=1}^{2}(Z_jR_{jk}+Z_{jk}R_j)\right)$$

  s.t. (15)
  Set $d_2^k=d_2^0$;
- *Step*-4: Make $P_{k+1}=P$, $L_{k+1}=L$, $Z_{j,k+1}=Z_j$, and $R_{j,k+1}=R_j$ $(j=1,2)$.

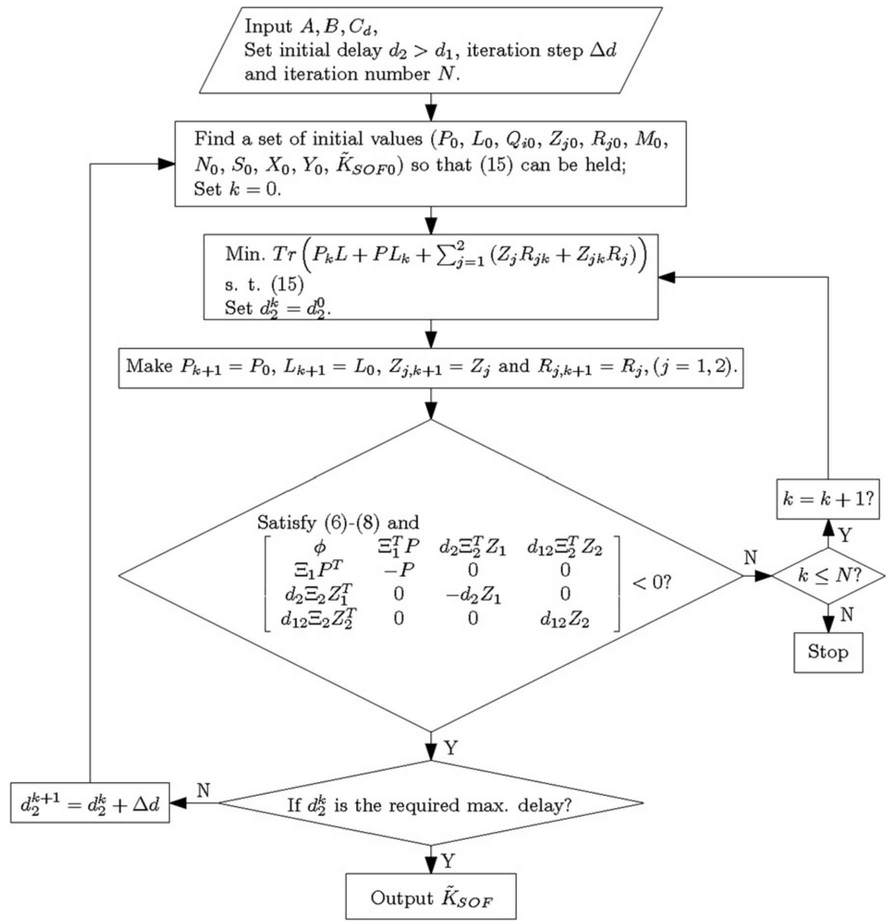


Fig. 2. Flowchart of the optimization algorithm for controller design.

- *Step*-5: If (6)–(8) can be held and the following LMI is feasible:

$$\begin{bmatrix} \phi & \Xi_1^TP & d_2\Xi_2^TZ_1 & d_{12}\Xi_2^TZ_2 \\ \Xi_1P^T & -P & 0 & 0 \\ d_2\Xi_2Z_1^T & 0 & -d_2Z_1 & 0 \\ d_{12}\Xi_2Z_2^T & 0 & 0 & d_{12}Z_2 \end{bmatrix} < 0$$

  then, set $d_2^{k+1} = d_2^k + \Delta d$; go to *Step*-2;
  else if $k > N$;
  stop the iteration;
  else
  $k = k+1$; go to *Step*-3;
  end
  end
- *Step*-6: Output the final results; End.

Fig. 2 shows the flowchart of the controller optimization. From this figure, it is clear that the time-varying delay of the wide area signal is considered during the controller design, which is helpful to find a suitable controller that can keep on an effective damping under the condition of time-varying delay on the wide area control signal.

4. Case-I: four-machine two-area test system with HVDC/AC interconnected lines

The four-machine two-area test system [17] is used to validate the presented controller design method. This system is divided into two areas where G1 and G2 are located in one area and G3 and G4 are located in the other area, as shown in Fig. 3. There are parallel AC/DC transmission lines to interconnect these two areas.

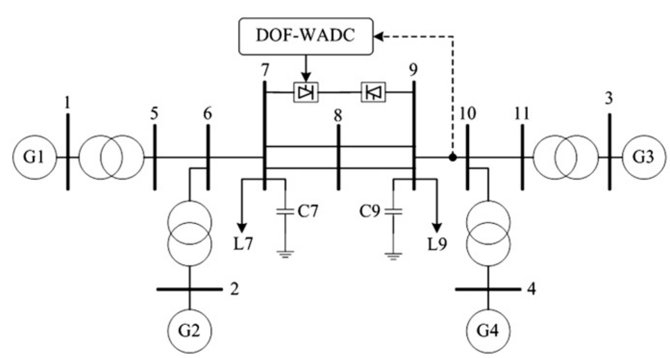


Fig. 3. Four-machine two-area test system with HVDC/AC interconnected lines.

This test system has a critical inter-area oscillation mode, which is represented as the generator oscillations between G1–G2 and G3–G4. Here, to damp this mode, the supplementary control of HVDC transmission is utilized to construct the DOF-WADC strategy. The control-input chooses the power flow in lines 9–10 and the control-output is the supplementary control-input of the converter pole controller at the rectifier side of HVDC transmission, as shown in Figs. 1 and 3.

A line-to-ground fault near bus 9 of lines 8–9, which starts at 1.0 s and is cleared after 0.1 s, is simulated to illustrate the

damping performance of the designed HVDC DOF-WADC when system suffers this big disturbance. Fig. 4 shows the dynamic response of the rotor speeds of the generators located in different areas. It can be seen that for the system without HVDC DOF-WADC, a big disturbance excites serious power oscillations among generators, as shown in Fig. 4(a). But when the system is installed with the HVDC DOF-WADC, the oscillations are damped effectively, as shown in Fig. 4(b).

Furthermore, Fig. 5 represents the dynamic response of the relative angle between G1 located in one area and G3 located in the other area. Fig. 6 represents the control-output response of the HVDC DOF-WADC. From these, it is clear that by means of the HVDC DOF-WADC, the inter-area oscillations are damped greatly. Besides, DOF-WADC can quickly respond to the oscillations and provide the effective control signal for oscillations damping.

Fig. 7 shows the dynamic response of power flow on tie-lines. From this, it can be seen that the big disturbance leads to serious power oscillations on the backbone transmission lines, which further makes system collapse. But when using HVDC DOF-WADC, the power oscillations are damped effectively. Therefore, the HVDC DOF-WADC strategy is good to the stable and security operation of interconnected system.

To investigate the effects of time-varying delay of wide area signal on the damping performance, various time delays, including the transmission delay and the signal-processing delay, are considered as a total delay. Fig. 8 shows the damping performance of the HVDC DOF-WADC under different time delays. It is clear that the designed controller can maintain good damping performance, though there exists a certain time-varying delay.

5. Case-II: sixteen-machine five-area test system with HVDC/AC interconnected lines

To further validate the effectiveness of the presented DOF-WADC, a more complex sixteen-machine five-area test system,

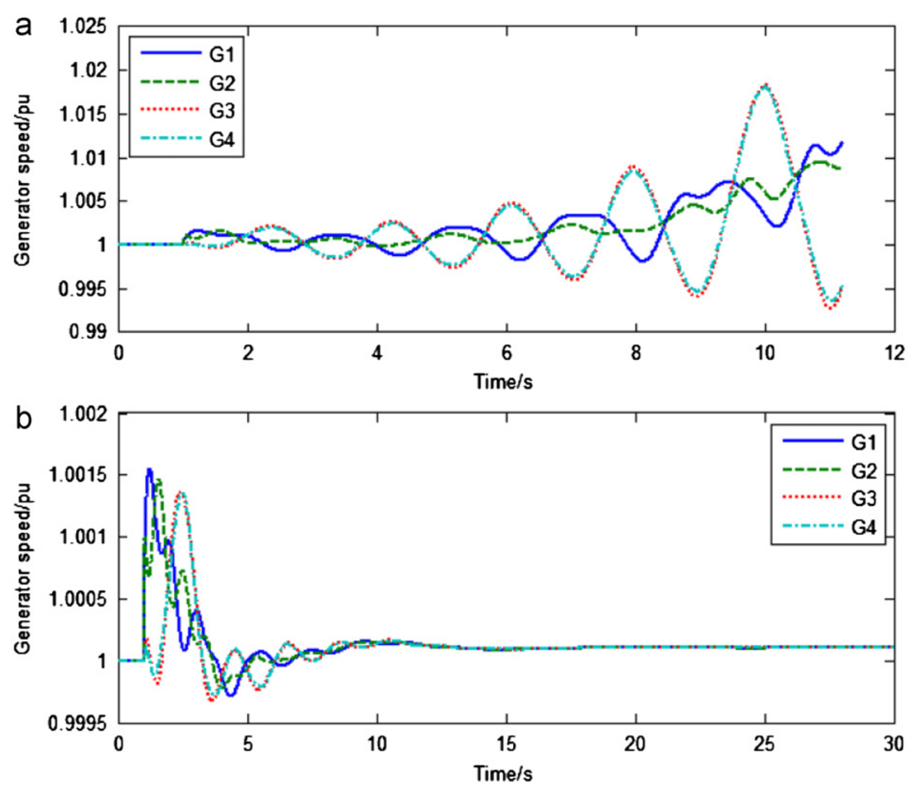


Fig. 4. Dynamic response of generator speed: (a) without HVDC DOF-WADC; (b) with HVDC DOF-WADC.

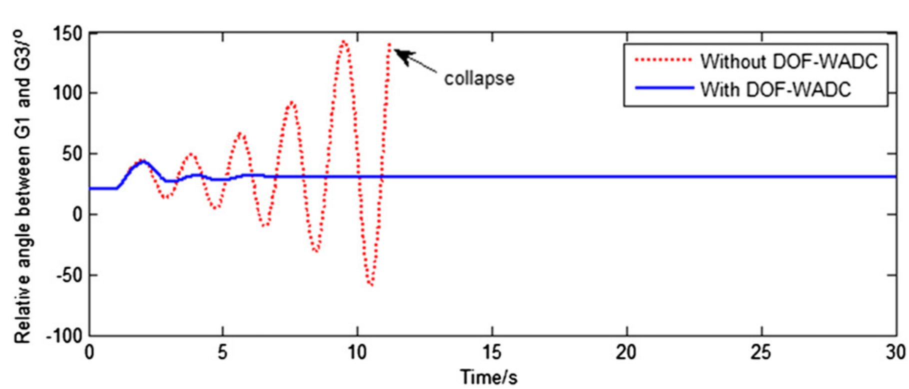


Fig. 5. Dynamic response of the relative angle between G1 and G3.

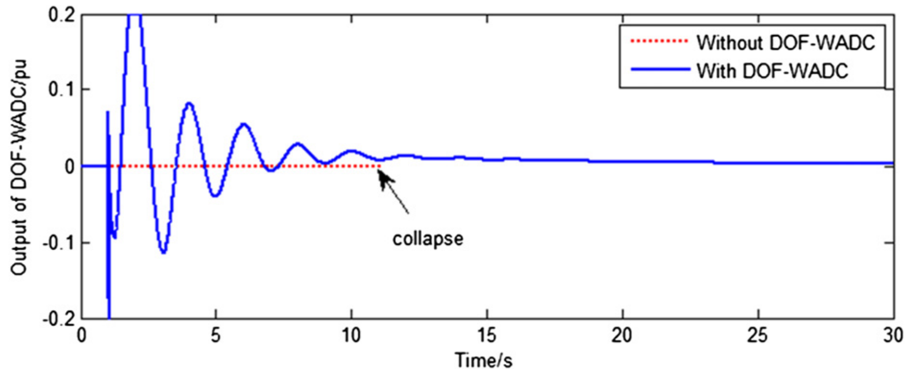


Fig. 6. Control-output of HVDC DOF-WADC.

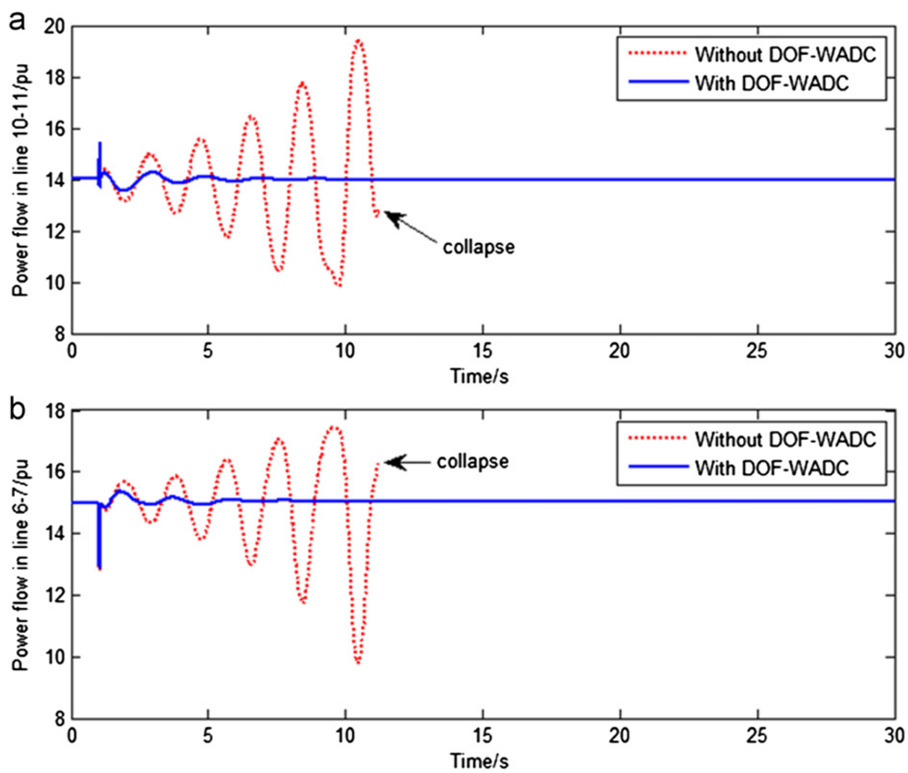


Fig. 7. Dynamic response of power flow: (a) lines 10–11; (b) lines 6–7.

that is the New England Test System (NETS) and the New York Power System (NYPS) interconnected system [17], shown in Fig. 9, is studied in detail.

5.1. *Choice of optimal wide area signal for DOF-WADC*

At the first, the modal analysis is carried out to reveal the inter-area oscillations. Fig. 10 shows the oscillation shape and the eigenvalues. On the nominal operating condition, this system has four typical inter-area modes, as shown in Fig. 10(b). Among these, there is a mode 1 with frequency $f = 0.5773$ Hz and small damping ratio $\rho = 0.0152$. Fig. 10(a) shows its oscillation shape, from which it can be seen that this mode is dominated by the oscillations between area 3 and areas 1 and 5.

The HVDC DOF-WADC is used to damp this critical mode. Here, power flow is candidate as the control-input. According to residue method, the damping contribution of power flow on each line of the test system can be obtained, as shown in Fig. 11. It can be see from this figure that compared to the local control signals, the wide area signal, that is the power flow in line 85 (see lines 52–68 in Fig. 9), can get the best control performance. Therefore, it is selected as the control-input of DOF-WADC.

5.2. *DOF-WADC design*

The order of the linearized model of this test system is 202, which is too high to be difficult for controller design within the LMI framework. Here, the balanced truncation model-reduction method is used to reduce the model order from 202 to 9. Fig. 12 shows the bode diagram of the full- and the reduced-order system. It is clear that over the wide frequency range ($10^{-3}-10^{4}$ Hz), the reduced-order system is very close to the full-order system, which indicates that the reduced-order system can fully reflect the dynamic characteristics of the full-order system.

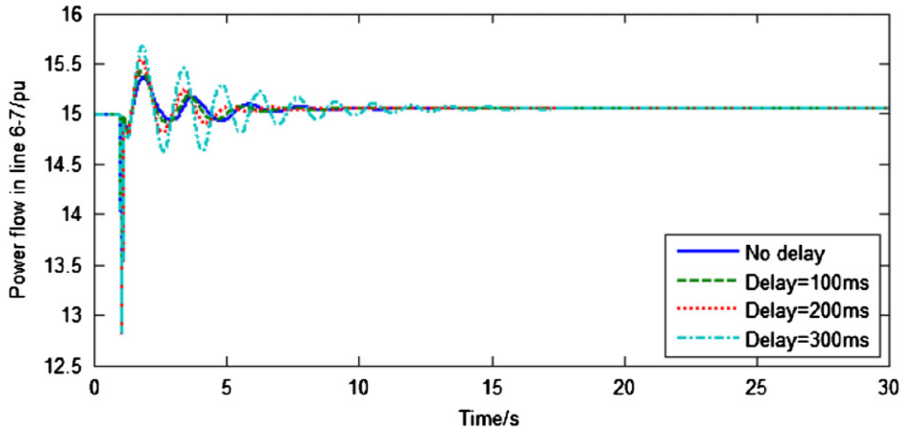


Fig. 8. Delay effect of wide area signal on damping performance of HVDC DOF-WADC.

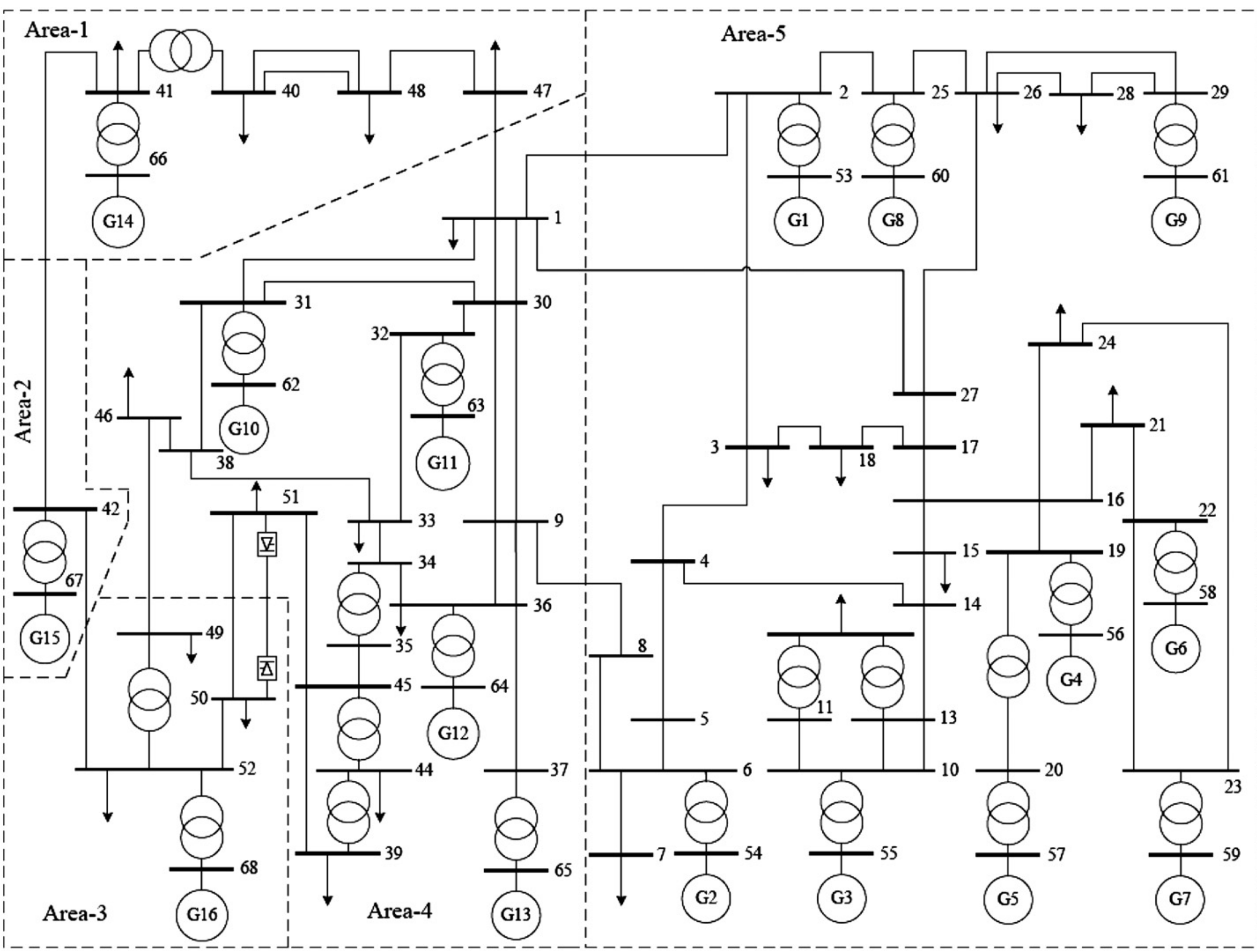


Fig. 9. Sixteen-machine five-area NETS–NYPS interconnected system with HVDC/AC interconnected lines.

According to the presented controller design method, the HVDC DOF-WADC for this test system can be obtained as follows:

$$u(k)=\begin{bmatrix} D_c & C_c \\ B_c & A_c \end{bmatrix} y(k)=\begin{bmatrix} 0.0282 & 0.6303 \\ -0.0024 & 0.9862 \end{bmatrix} y(k). \tag{16}$$

Furthermore, Fig. 13 gives the root locus of the test system which adopts the above controller (16) with different overall control gain. From this figure, it can be seen that the designed controller represents a good response performance to the considered inter-area mode. It can greatly move this mode (small damping ratio, $\rho < 0.05$) to the left-plane, which means the improvement of the system stability.

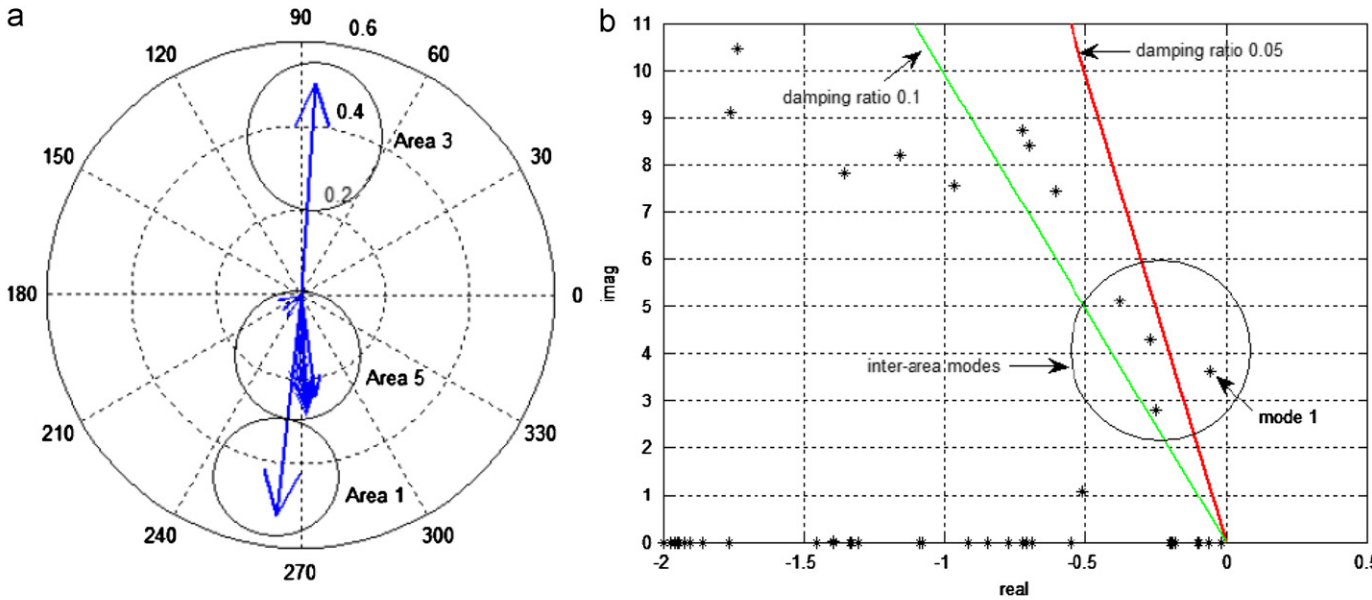


Fig. 10. Inter-area mode with small damping ratio ($\rho < 0.05$): (a) oscillation shape; (b) eigenvalues.

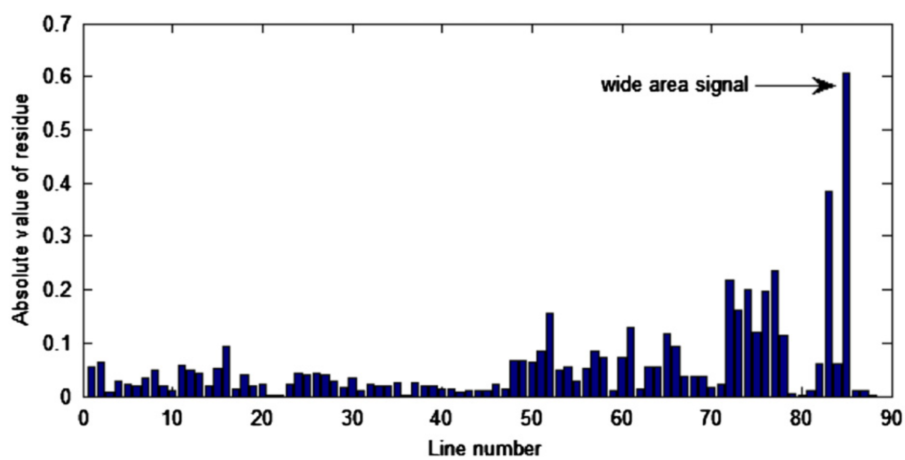


Fig. 11. Damping contribution of different line flow as the control-input of DOF-WADC.

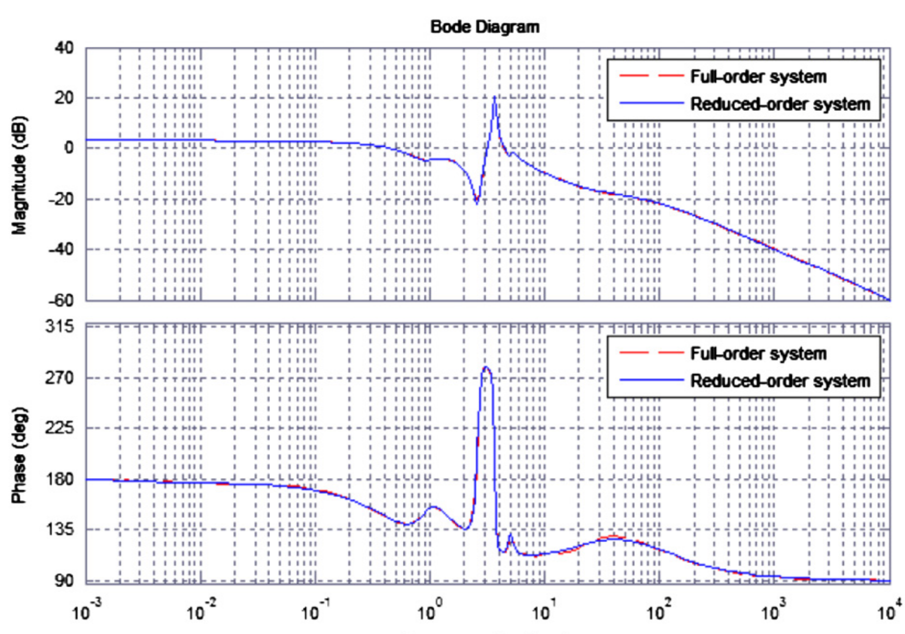


Fig. 12. Comparison of bode diagram of the full- and the reduced-order system.

5.3. Nonlinear simulation

In order to evaluate the damping performance of the presented DOF-WADC, the nonlinear simulation is performed, which includes the controller evaluation on different operating conditions (e.g., line-to-ground fault and line outage).

5.3.1. Line-to-ground fault

A line-to-ground fault near bus 1 of lines 1–2 is considered to test the performance of the designed HVDC DOF-WADC. Fig. 14 shows the dynamic response of the relative angle between generators located in different areas. From this figure it can be seen that the designed controller can effectively damp the inter-area oscillations within 15 s. Fig. 15 gives the control-output, which also indicates that the controller has a quick response for oscillation damping. Furthermore, Fig. 16 represents the power flow on the tie-lines, which indicates that the power oscillations on the backbone transmission lines are damped effectively.

Besides, to evaluate the damping performance under time-varying delay of wide area signal, Fig. 17 further gives the

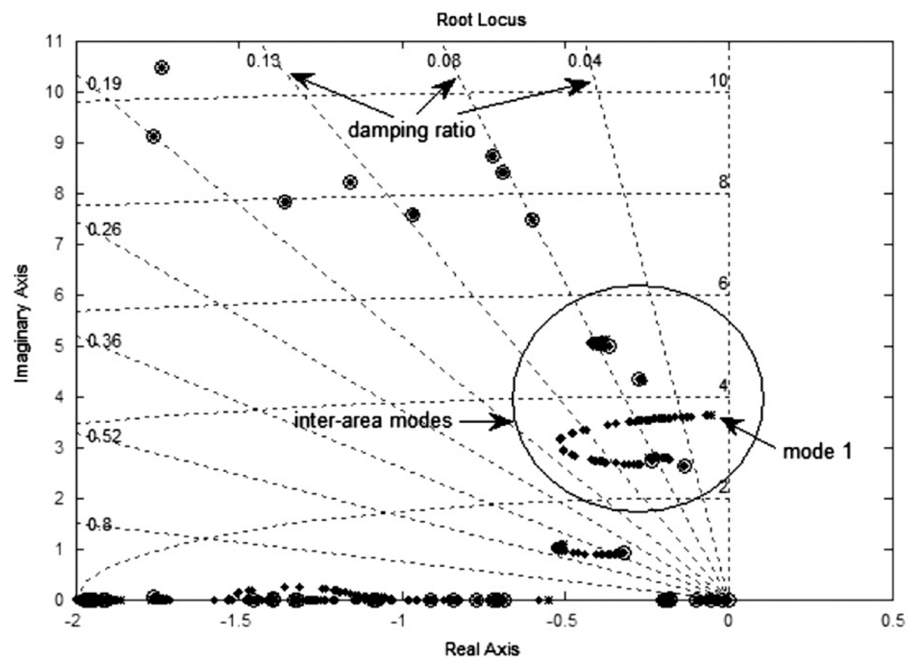


Fig. 13. Root locus diagram of the test system under the action of the DOF-WADC.

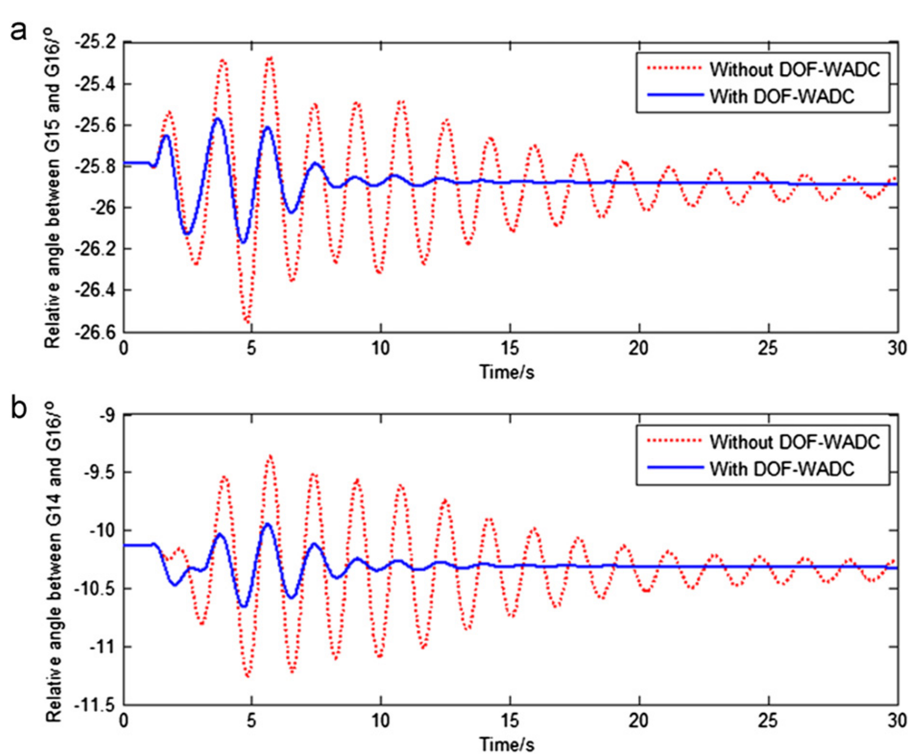


Fig. 14. Dynamic response of relative angle: (a) between G15 and G16; (b) between G14 and G16.

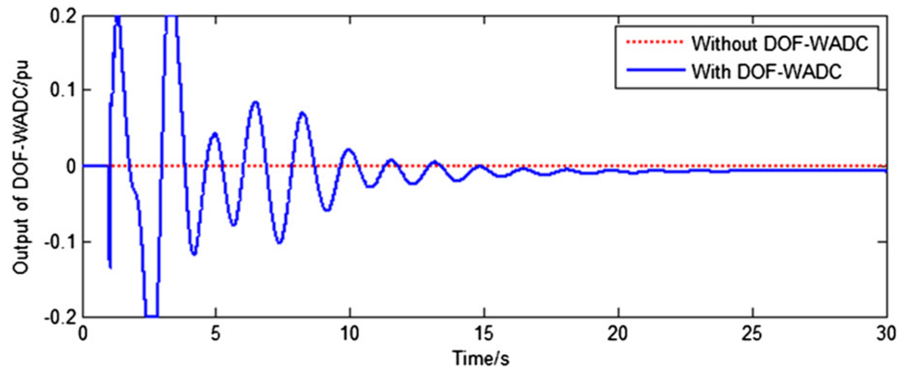


Fig. 15. Control-output response of DOF-WADC to a line-to-ground fault.

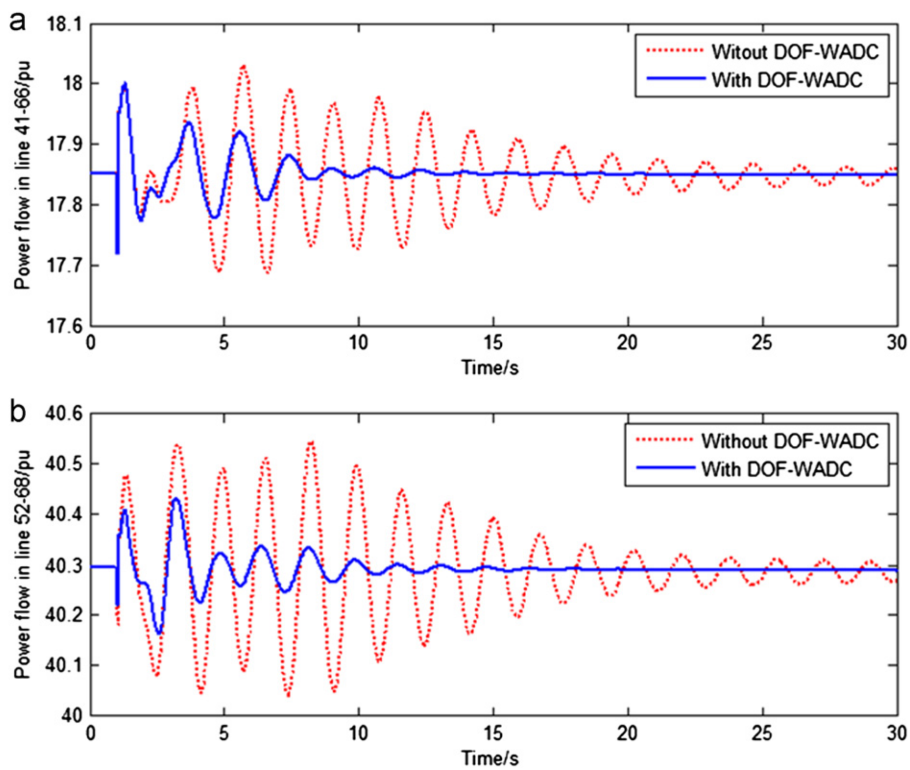


Fig. 16. Dynamic response of power flow in the tie-lines: (a) lines 41–66; (2) lines 52–68.

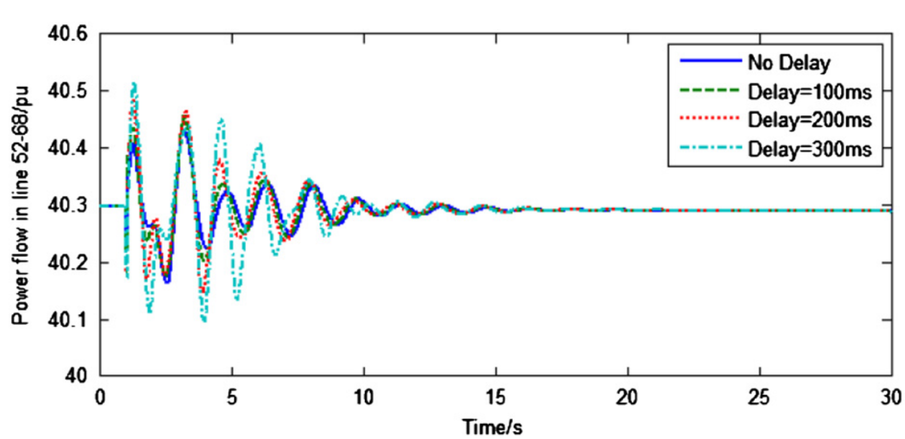


Fig. 17. Time-varying delay effect of wide area signals on damping performance of DOF-WADC.

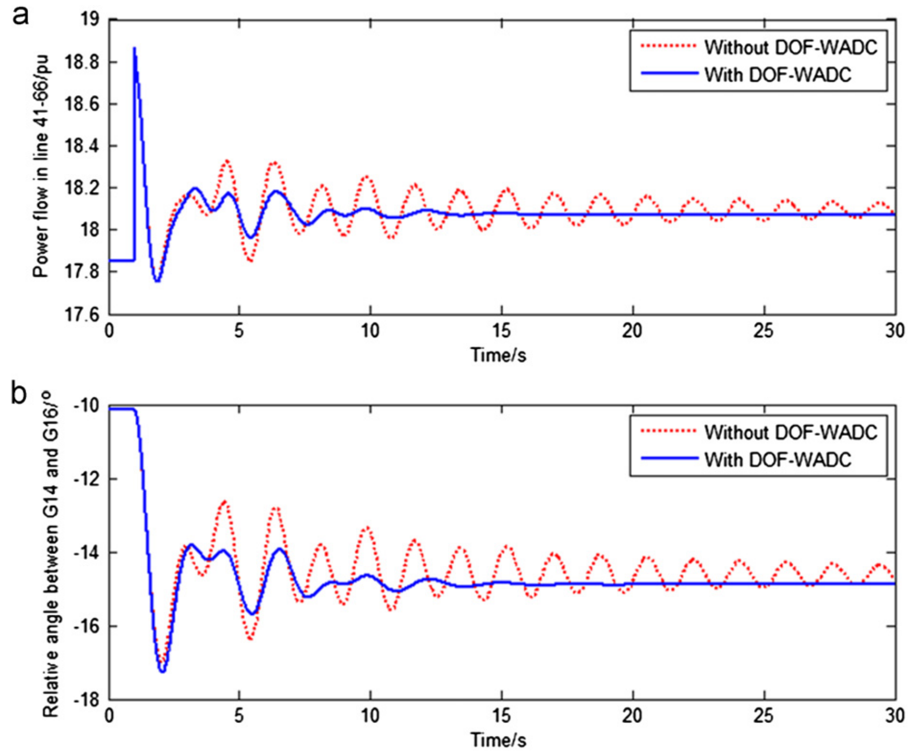


Fig. 18. Dynamic response of the test system to a line outage: (a) power flow in lines 41–66; (b) relative angle between generators.

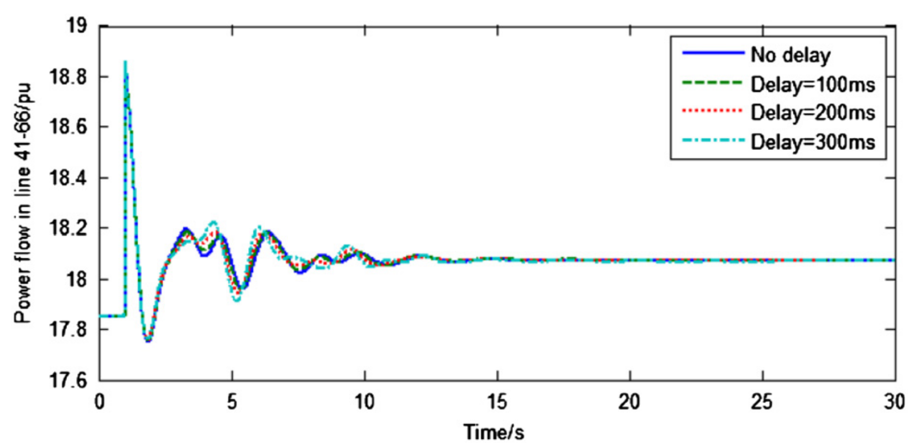


Fig. 19. Dynamic response of the test system under different time delays of wide area signal.

dynamic response of the power flow in lines 52–68. It is clear from this figure that although it has different time delays for the wide area signals, the designed DOF-WADC still maintains a good damping performance, which illustrates the effectiveness and the reliability of the presented controller design method.

5.3.2. Line outage

The outage of interconnected lines 1–47 is considered to further test the DOF-WADC under different operating conditions. Fig. 18 shows the dynamic responses of the test system to such line outage. From both the power flow from the transmission side and the relative angle from the generation side, it is clear that the designed controller still keeps on a good damping performance under this operating condition. Moreover, Fig. 19 gives the dynamic responses of the test system under different time delays of wide area signals. It is also clear that the DOF-WADC maintains a good damping performance even when the wide area signal exists various time delays.

6. Conclusion

This paper proposed a DOF-WADC and related controller design method to damp inter-area oscillations and thus to enhance the stability of large-scale power systems with parallel HVDC/AC interconnected lines. This method can sufficiently utilize the supplementary control function of HVDC transmission, and implement an effective wide area damping control through introducing a suitable wide area signal. By employing an advanced stabilization theorem, the design problem of DOF-WADC is formulated as a standard nonlinear optimization problem with a set of LMI constrains. An iterative algorithm is correspondingly presented to solve the controller parameters

within the LMI framework. The time-varying delay of wide area signals is considered during the process of controller design. Unlike the conventional SOF control that only has a single constant control gain, in this paper, the WADC has a good dynamic damping performance, and it is represented as a dynamic SS form. Two case studies validated this control method, and revealed the good damping performance when applied in power systems with parallel HVDC/AC interconnected lines.

References

[1] Bahrman MP. HVDC transmission overview. In: Proceedings of the 2008 IEEE/PES transmission and distribution conference and exposition; 2008. p. 1–7.
[2] Ohrem S, Ringelband T, Moser A. Coordinated operation of HVDC systems in extra-high voltage networks. In: Proceedings of the 2010 IEEE power and energy society general meeting; 2010. p. 1–5.
[3] Povh D, Thepparat P, Westermann D. Analysis of innovative HVDC control. In: Proceedings of the 2009 IEEE Bucharest PowerTech; 2009. p. 1–7.
[4] Cai JY, Huang ZY, Hauer J, Martin K. Current status and experience of WAMS implementation in North America. In: Proceedings of the IEEE/PES Asia and Pacific transmission and distribution conference and exhibition. p. 1–7.
[5] Hauer JF, Mittelstadt WA, Martin KE, Burns JW, Lee H, Pierre JW, et al. Use of the WECC WAMS in wide-area probing tests for validation of system performance and modeling. IEEE Transactions on Power Systems 2009;24(February (1)):250–7.
[6] Zima M, Larsson M, Korba P, Rehtanz C, Andersson G. Design aspects for wide-area monitoring and control systems. Proceedings of IEEE 2005;93(May 5):980–96.
[7] Vournas CD, Metsiou A, BM. Nomikos, Analysis of inter-area and interarea oscillations in South-Eastern UCTE interconnection. In: Proceedings of the 2009 IEEE Power and Energy Society General Meeting; 2009. p. 1–7.
[8] Xiao-ming M, Yao Z, Lin G, Xiao-chen W. Coordinated control of interarea oscillation in the China Southern power grid. IEEE Transactions on Power Systems 2006;21(May (2)):845–52.
[9] Wu H, Tsakalis KS, Heydt GT. Evaluation of time delay effects to wide-area power system stabilizer design. IEEE Transactions on Power Systems 2004;19(November (4)):1935–41.
[10] Zarghami M, Crow ML, Jagannathan S. Nonlinear control of FACTS controllers for damping interarea oscillations in power systems. IEEE Transactions on Power Delivery 2010;25(October (4)):3113–21.
[11] Nguyen H, Dessaint L, Okou AF, Kamwa I. A power oscillation damping control scheme based on bang–bang modulation of FACTS signals. IEEE Transactions on Power Systems 2010;25(November (4)):1918–27.
[12] Stahlhut JW, Browne TJ, Heydt GT, Vittal V. Latency viewed as a stochastic process and its impact on wide area power system control signals. IEEE Transactions on Power Systems 2008;23(February (1)):84–91.
[13] Chaudhuri B, Majumder R, Pal BC. Wide-area measurement-based stabilizing control of power system considering signal transmission delay. IEEE Transactions on Power Systems 2004;19(November (4)):1971–9.
[14] Xu S, Lam J. Improved delay-dependent stability criteria for time-delay systems. IEEE Transactions on Automatic Control 2005;50(March (3)):384–7.
[15] Wu M, Liu F, Shi P, He Y, Yokoyama R. Stability analysis for discrete-time recurrent neural networks with time-varying delay. IEEE Transactions on Circuits and Systems, II 2008;55(7):600–4.
[16] Farsangi MM, Song YH, Lee KY. Choice of FACTS device control inputs for damping inter-area oscillations. IEEE Transactions on Power Systems 2004;19(May (2)):1135–43.
[17] Rogers G. Power system oscillations. Norwell, MA: Kluwer; 2000.
[18] Gahinet P, Nemirovski A, Laub A, Chilali M. LMI control toolbox for use with matlab. The Math Works Inc.; 1995.
[19] El Ghaoui L, Oustry F, AitRami M. A cone complementarity linearization algorithm for static output-feedback and related problems. IEEE Transactions on Automatic Control 1997;42(August (8)):1171–6.